SHOCK TUBE SPECTROSCOPY LABORATORY

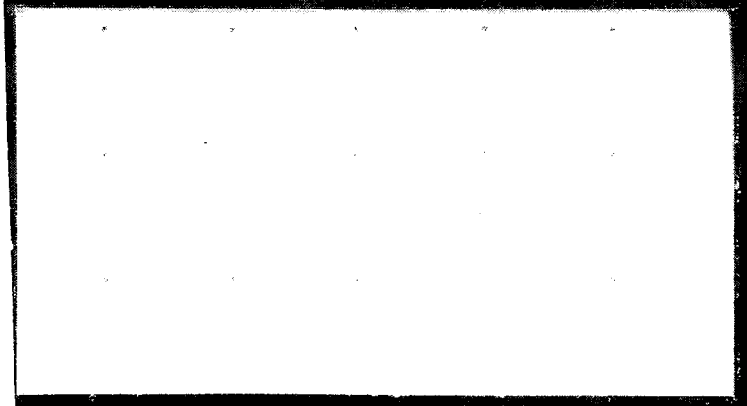

HARVARD COLLEGE OBSERVATORY

60 GARDEN STREET

CAMBRIDGE, MASS

THE CONTRIBUTION OF PERTURBER RADIATION TO THE SHAPES OF SPECTRAL LINES BROADENED BY ELECTRON IMPACTS

D.D. Burgess*

Scientific Report No. 29

Harvard College Observatory, Cambridge, Mass. U.S.A.
and
Physics Department, Imperial College of Science and Technology
London, England

July 1968

* On leave-of-absence at Harvard College Observatory, 1967-68.

Abstract

Theories of electron impact broadening have previously neglected the radiation produced by the perturbing electrons. In this paper a theory is developed to take the perturber radiation into account, and so to evaluate possible interference terms. These may lead to observable asymmetries of lines of ionized emitters.

I. INTRODUCTION

The treatment of the electron impact broadening of spectral lines emitted by ionized species in a plasma has recently been the subject of much attention[1-5]. Discrepancies of up to an order of magnitude between experimental line-widths and the predictions of earlier classical path theories[3] have been attributed to the use of straight rather than hyperbolic classical paths in the theory[6], the importance of perturber energies close to threshold for inelastic collisions[1,2], and the importance in many cases of lower state interactions. Various attempts have been made to modify the existing theory appropriately[1,2]. Simultaneously, the advent of sources of high temperature plasma of extreme density, particularly plasmas generated with high power laser beams, has allowed observations of electron impact broadening to be extended to ionization stages as high as the ninth[6].

An approximation made in all previous theories, which needs reconsideration if the lines of interest are emitted by ions, is the neglect of the coupling between the external radiation field and the perturbing electrons. This approximation is inherent in the classical path theory[3]

and is also made in the relaxation theory[7], which distinguishes between the absorbing 'system' (an atom or ion) and the surrounding plasma 'bath'. Bezzerides[8] has recently given a theory of line-broadening using the temperature - Green's function technique. In principle the radiation-perturber coupling could be included within this approach by considering explicit contributions to the photon propagator. However, Bezzerides' expression of the line-shape in terms of a two-particle atom-hole propagator effectively ignores such effects. The use in his theory of distinct propagators for perturbing electrons and for 'atoms' (the latter including both translational motion and internal excitation) is appropriate in considering the broadening of lines of neutral atoms, but is very much less convenient when both bound and free electrons interact primarily with the field of the same, highly charged, ion.

The present paper develops a theory which treats the bound and perturbing electrons on an equal footing in so far as their coupling to the radiation field is concerned. The resultant absorption cross-section contains interference terms which can cause observable asymmetries of otherwise Lorentzian line-profiles. These asymmetries have a formal similarity to those observed in the profiles of lines due to

transitions to autoionizing states in unperturbed atoms, since both cases involve an interference between two possible decay channels of a system.

II. FORMULATION

The cross-section for absorption of a photon by a system can be written in terms of the diagonal elements of the transition operator, T:

$$\sigma = -\frac{2}{\hbar F}\,\mathrm{Im}\sum_i T_{ii} \qquad (1)$$

$$\left(= \frac{2\pi}{\hbar F}\sum_{f\neq i}\delta(E_f - E_i)\,|T_{fi}|^2 \right)$$

where F is the photon flux (see e.g. Ref. 9). This expression neglects some effects of the medium by assuming that the internal and external fields are identical. We shall also neglect Doppler-shift and recoil effects. In most electron broadening problems the errors produced are negligible.

The evaluation of σ, which would otherwise be a many-body problem, is made possible by the one-electron approximation[4,5,10].

Baranger[10] has shown that, if the impact approximation[3,10] holds for frequency separations from the line center as large as one-line width, Γ, then the line wings at separations greater than Γ can be treated as if each absorber interacted only with a single perturber. The system of interest then consists simply of one atom or ion, one perturber, and a photon. The criteria necessary for this approximation to be valid usually hold in electron broadening problems, and since the region of interest in this paper is the line-wing, the one-electron approximation will be adequate. A generalization to the line-core, treating the many-perturber case in the impact approximation, is given later.

The Hamiltonian of the simplified system is written as H, where:

$$H = H^\circ + H' \tag{2}$$

$$H^\circ = H^\circ(\text{ion}) + \frac{p^2}{2m} - \frac{Ze^2}{r_a} + H^\circ(\text{rad}) \tag{3}$$

$$H' = V^{\text{int}} + V^{\text{rad}} \tag{4}$$

$$V^{\text{rad}} = \frac{e}{mc}\sum_j P_j \cdot A(r_j) + \frac{e^2}{2mc^2}\sum_j A^2(r_j) \tag{5}$$

Although widely used in line-broadening problems, this expansion may be of doubtful utility in some instances. However, it is entirely adequate for present purposes, since we are interested in evaluating the relative contributions of various terms, and if necessary this can be done order by order.

Baranger[10] has calculated the line-width in the one-electron approximation by using the Born expansion of the T-matrix, and the alternative prescription of calculating the sum of the squares of the off-diagonal elements. He considered elements deriving from only one order in the expansion of T, and obtained a Lorentz line-shape. This neglects other contributions to σ, which are more apparent if we consider the diagonal elements of T, and which, although usually small, are of lower order than those yielding the Lorentz shape. The expression of σ in terms of the diagonal elements of T is also nearer to the form of the many-body technique[8], and simplifies the averaging over perturber states and over angles. Baranger's cross-section is identical to one of the three terms considered below.

Diagrammatic Representation of T_{ii}

The physical processes of interest, i.e. the various alternative orderings of V^{rad} and V^{int} in (8), are conveniently represented in diagrammatic form, Figure 1. Each solid line represents either a bound or a perturbing electron in an eigen state of H°. Since these are Coulomb states, the emission or absorption of radiation requires only a single vertex, representing a matrix element of the interaction V^{rad}. The interaction between the electrons, V^{int}, is shown by a dotted line. The diagrams in which both photon lines intersect a bound electron line correspond to line radiation (including the usual broadening processes) and those with both V^{rad} interactions in a 'free' electron line represent continuum radiation (hydrogenic bremsstrahlung, 2(A), plus corrections due to the presence of the bound electron). We are interested here in a third class, e.g. 3(A), which is mixed in the sense that one photon vertex occurs in the bound line and one in the 'free' line. These diagrams occur essentially because both bound and free electrons move in the field of the same ion.

The interpretation of the diagrams is straightforward. Each vertex contributes the appropriate matrix element of V^{rad} or V^{int}. A factor G is associated with each region between

two vertices. Thus, if the bound and free electrons are in states b and β respectively, the factor is $G^{b\beta}$, where:

$$G^{b\beta}(\omega) = < b\beta \left| \frac{1}{E_i - H^\circ + i\eta} \right| b\beta > \tag{9}$$

$$E_i = E_{a\alpha\gamma} = < a\alpha\gamma | H^\circ | a\alpha\gamma > = E_a + E_\alpha + \hbar\omega \tag{10}$$

$$\sum_{b\beta} G^{b\beta} = \sum_{E_{b\beta} \neq E_i} \frac{1}{(E_i - E_{b\beta})} - i\pi\, \delta(E_i - E_{b\beta}) \quad . \tag{11}$$

Finally, the statistical average is carried out by associating a factor ρ_α with the initial perturber state α, and then summing over α. Thus, for example the expression corresponding to 3(A) reads:

$$T_{ii}^{3(A)} =$$

$$\sum_{b\alpha\beta} \rho_\alpha < a\alpha\gamma | V^{*rad} | a\beta > G^{a\beta} < a\beta | V^{int} | b\alpha > G^{b\alpha} < b\alpha | V^{rad} | a\alpha\gamma > \tag{12}$$

The diagonal nature of the T-matrix elements required in determining σ can be emphasized by joining the initial and final lines for the free and bound electrons. The

resulting 'bubble' diagrams (Figure 2) are both more succinct, and in closer correspondence to Bezzerides' theory[8]. The usual rules of graphical perturbation theory[11] then apply to their interpretation, except that the energy of each state is taken as being that of a state of H°, and a weighting factor σ_α is introduced in lieu of using temperature Green's functions. Figure 3 illustrates the relationship between the present diagrams, and the more complicated diagrams that would result if the more usual free particle states had been employed instead of the Coulomb states used in Figures 1 and 2.

III. CONTRIBUTIONS FROM SPECIFIC DIAGRAMS

We now consider the contributions to the absorption cross-section of diagrams 1(B), 1(C), and 3(A). 1(D) and 3(B), (C), (D) can be shown to contribute with the same sign as 1(C) and 3(A), and will be included only in the final discussion. 2(A) gives the usual Bremsstrahlung cross-section without difficulty and is not explicitly considered. The contribution to σ of each of these diagrams is proportional to the number density of the perturbing electrons, n_e, and of ions in the ground state, n_a. n_e and n_a will therefore be set equal to unity throughout.

Interaction Matrix Elements

We write V^{int} as a multipole expansion:

$$V^{int} = \frac{e^2}{r_{12}} - \frac{e^2}{r_2} = e^2\left\{ \sum_{k=0}^{k=\infty} \frac{r_<^k}{r_>^{k+1}} \; C^k(1) \cdot C^k(2) - \frac{1}{r_2} \right\} . \quad (13)$$

Matrix elements of V^{int} are therefore of the form

$$\langle a\alpha|V^{int}|b\beta\rangle = e^2\left\{ \sum_{k=0}^{k=\infty} R^k(a\alpha,b\beta) \langle a\alpha|C^k(1)\; C^k(2)\,|b\beta\rangle - \langle a\alpha|\frac{1}{r_2}|b\beta\rangle \right\} \quad (14)$$

where $R^k(a\alpha,\ b\beta)$ and C^k have their usual meanings, for instance as given by Shore and Menzel[12].

In most cases of interest in line-broadening, we obtain a very good approximation by neglecting that part of the generalized Slater integral $R^k(a\alpha,\ b\beta)$ where $r_2 < r_1$, and by assuming instead simply that $r_2 \equiv r_>$. Then the matrix element in $\frac{e^2}{r_2}$ exactly cancels the monopole ($k = 0$) contribution in the summation over k, and we can simplify the expression for V^{int} to:

$$\langle a\alpha|V^{int}|b\beta\rangle = e^2 \sum_{k=1}^{k=\infty} R^k(a\alpha,b\beta) \langle a\alpha|C^k(1) \cdot C^k(2)\,|b\beta\rangle . \quad (15)$$

In this approximation exchange contributions vanish.

The matrix elements of V^{rad} are written in terms of tensor operators in an exactly similar way and we retain only the dipole contributions. Then:

$$< a(1)\alpha(2)\,\gamma|V^{rad}_{(1)}|b(1)\beta(2)> = \gamma_1 < a(1)\alpha(2)\,|C^1_m(1)\,|b(1)\alpha(2)> I(a,b) \tag{16}$$

where

$$I(a,b) = \int_0^\infty P_a(r)\; r\; P_b(r)\; dr \tag{17}$$

and γ_1, the constant appropriate to electric dipole radiation, is:

$$\gamma_1 = \left(\frac{2\omega^3}{3c^3\eta}\right)^{\frac{1}{2}} \quad \text{with the flux,} \quad F = \frac{\omega^2}{3\pi^2 c^2} \quad . \tag{18}$$

Evaluation of the Matrix Elements Corresponding to Each Diagram

The expressions for the three contributions of interest can now be written out:

$$T_{ii}^{1(B)}(\omega) = -\sum_{\substack{b,\alpha,\beta \\ k,m}} (\gamma_1)^2 e^4 \, n_\alpha (G^{b\alpha})^2 \; I(a,b)^2 \; R^k(b\alpha,b\alpha)$$

$$\times \left[\langle a(1)\alpha(2) \; | C_m^1(1)^* | b(1)\alpha(2) \rangle \langle b \; \alpha | C^k(1) \cdot C^k(2) | b\alpha \rangle \langle b \; \alpha | C_m^1(1) | a \; \alpha \rangle \right] \tag{19}$$

$$T_{ii}^{1(C)}(\omega) = -\sum_{\substack{b,b',\alpha,\beta \\ k,k',m}} (\gamma_1)^2 e^6 \, n_\alpha (G^{b\alpha})^2 G^{b'\beta} (I(a,b)^2 \; R^k(b\alpha,b'\beta) R^{k'}(b'\beta,b\alpha)$$

$$\times \left[\langle a\alpha | C_m^1(1)^* | b\alpha \rangle \langle b\alpha | C^k(1) \cdot C^k(2) | b'\beta \rangle \langle b'\beta | C^{k'}(1) \cdot C^{k'}(2) | b\alpha \rangle \langle b\alpha | C_m^1(1) | a\alpha \rangle \right] \tag{20}$$

$$T_{ii}^{3(A)}(\omega) = -\sum_{\substack{b,\alpha,\beta \\ k,m}} (\gamma_1)^2 e^4 \, n_\alpha G^{b\alpha} G^{a\beta} I(a,b) I(\beta,\alpha) \; R^k(b\alpha,a\beta)$$

$$\times \left[\langle a\alpha | C_m^1(2)^* | a\beta \rangle \langle a\beta | C^k(1) \cdot C^k(2) | b\alpha \rangle \langle b\alpha | C_m^1(1) | a\alpha \rangle \right] \tag{21}$$

In each case the expression is broken into two parts. The square brackets contain the angular dependence, both of the summation over intermediate states and of the average over initial emitter-perturber orientations. The remaining part contains the averages and summations over the initial and intermediate energies and momenta of the perturbing electron, and over the intermediate energies of the bound electron.

The Angular Average

Previous electron-impact broadening theories have either carried out the angular average classically[3] or have used the properties of the 3-j symbols, together with a coordinate rotation[4] (in the classical path case), or a summation over appropriate quantum numbers in a representation in which the angular momenta of bound and perturbing electrons are uncoupled[10]. However, the analysis can be considerably shortened by using a coupled representation chosen to diagonalize V^{int}. The summation properties of the 6-j symbols[12] then make the angular average particularly succinct.

The single-particle perturber states we use in constructing the basis of the coupled representation are the well-known Coulomb wave functions for an electron of momentum $\hbar K$, decomposed into partial waves, for instance as given by Alder et al.[13]. An outgoing wave is then:

$$|K_\beta\rangle = 4\pi \sum_{\ell m} i^\ell \, e^{-i\sigma(\ell, E_\beta)} \, Y^*_{\ell m}(\Omega) Y_{\ell m}(\theta,\phi) \, \frac{F_\ell(Kr)}{Kr} \quad . \tag{22}$$

This function is normalized to unit particle density and to:

$$\langle K'|K\rangle = (2\pi)^3 \, \delta(K-K') \quad . \tag{23}$$

Since for the present problem the perturber momentum, $\hbar K$, is distributed isotropically with respect to the (arbitrary) direction of quantization, and since the summation over each intermediate state introduces a term of the form:

$$\int Y^*_{\ell m}(\Omega) \; Y_{\ell m}(\Omega) \; d\Omega = 1, \tag{24}$$

we may directly integrate over all perturber angles, Ω, and ignore the $Y_{\ell m}(\Omega)$ factors from now on. We need make no

distinction between incoming and outgoing waves in the initial or intermediate states, since the relevant factors in $|k><k|$ just cancel. (Note that the immediacy of these simplifications is a result of using the diagonal rather than the off-diagonal elements of T in obtaining σ.)

We are left simply with a normalized product of radial and angular functions, and instead of product states we may immediately use coupled states. The choice of a coupling scheme diagonalizing V^{int}, which is essentially the electrostatic interaction, is obvious from the usual theory of atomic spectra[12]. In line-broadening problems, where the energy and angular momenta of the perturbing electrons are usually high, the most 'physical' choice is the $j_1(K)$ scheme.

The details will be given only for the contribution to the cross-section corresponding to diagram 3(A), the development being similar in the other cases. Note that since the initial-emitter perturber orientations are isotropically distributed, this average is carried out simultaneously with the summation over the intermediate quantum numbers.

The angular part of (21) is:

$$A^{3(A)} = \sum_{\substack{MM'M" \\ JJ' \\ KK'}} < j_1,\ell_2(K)JM|C^{1*}_q(2)|j_1\ell_2'(K")J"M" >$$

$$x < j_1\ell_2'(K")J"M"|C^k(1)\cdot C^k(2)|j_1'\ell_2(K')J'M >$$

$$x < j_1'\ell_2(K')J'M'|C^1_q(1)|j_1,\ell_2(K)JM > \qquad (25)$$

We proceed by first writing out the M-dependence explicitly in terms of 3-j symbols, using $(C^k_q)^* = (-1)^q C^k_{-q}$, and $q = M - M'$:

$$A = \sum_{\substack{MM'q \\ JJ' \\ KK'}} (-1)^{J-M}(-1)^{J'-M'}(-1)^{M'-M} \begin{pmatrix} J' & 1 & J \\ -M' & -q & M \end{pmatrix} \begin{pmatrix} J & 1 & J' \\ -M & q & M' \end{pmatrix} \frac{\delta_{M'M"}}{\sqrt{2}} \frac{\delta_{J'J"}}{\sqrt{2K'+1}}$$

$$x < j_1\ell_2(K)J\|C^1(2)\|j_1\ell_2'(K')J'><j_1\ell_2'(K')\|C^k(1)\cdot C^k(2)\|j_1'\ell_2(K") >$$

$$x < j_1'\ell_2(K")J"\|C^1(1)\|j_1\ell_2(K)J > \qquad (26)$$

Carrying out the summation over M and M' we next write out the expression in terms of matrix elements fully reduced to the

uncoupled scheme:

$$A = \sum_{\substack{JJ' \\ KK'}} \left[\frac{1}{\sqrt{2}} \frac{1}{\sqrt{2K+1}} (-1)^{J+3J'} \right]$$

$$\times \left[(2J+1)(2J'+1)(-1)^{K+\frac{1}{2}+J'+1} (-1)^{K''+\frac{1}{2}+J'+1} \begin{Bmatrix} \frac{1}{2} & K & J \\ 1 & J' & K' \end{Bmatrix} \begin{Bmatrix} \frac{1}{2} & K'' & J' \\ 1 & J & K \end{Bmatrix} \right]$$

$$\times \left[\sqrt{(2K'+1)} \; (-1)^{K'+\ell_2'+j_1'} \begin{Bmatrix} K' & \ell_2' & j_1 \\ k & j_1' & \ell_2 \end{Bmatrix} \right]$$

$$\times \left[(2K+1)(2K'+1)(-1)^{j_1+\ell_2'+K+1} (-1)^{j_1'+\ell_2+K+1} \begin{Bmatrix} j_1 & \ell_2 & K \\ 1 & K' & \ell_2' \end{Bmatrix} \begin{Bmatrix} \ell_2 & j_1' & K' \\ 1 & K & j_1 \end{Bmatrix} \right]$$

$$\times \langle \ell_2 \| C^{1} \| \ell_2' \rangle \langle \ell_2' \| C^{k} \| \ell_2 \rangle \langle j_1 \| C^{k} \| j_1' \rangle \langle j_1' \| C^{1} \| j_1 \rangle \qquad (27)$$

where each term in square brackets represents a different stage in the reduction process. Use of the summation properties[12]:

$$\sum_{j_3} (2j_3+1) \begin{Bmatrix} j_1 & j_2 & j_3 \\ j_4 & j_5 & j_6 \end{Bmatrix} \begin{Bmatrix} j_4 & j_5 & j_3 \\ j_1 & j_2 & j_7 \end{Bmatrix} = \frac{\delta_{j_6 j_7}}{(2j_6+1)} \qquad (28)$$

and

$$\sum_{j_3} (-1)^{j_3+j_6+j_7} (2j_3+1) \begin{Bmatrix} j_1 & j_2 & j_3 \\ j_4 & j_5 & j_6 \end{Bmatrix} \begin{Bmatrix} j_4 & j_5 & j_3 \\ j_2 & j_1 & j_7 \end{Bmatrix} = \begin{Bmatrix} j_1 & j_5 & j_6 \\ j_2 & j_4 & j_7 \end{Bmatrix} \tag{29}$$

repeatedly in carrying out the summations over J, J', K, K' (in that order) then finally yields:

$$A = (-1)^{2J}(-1)^{j_1+j_1'} \frac{\sqrt{2}}{(2k+1)} \delta_{kl} \langle j_1 \| C^1 \| j_1' \rangle \langle j_1' \| C^1 \| j_1 \rangle$$

$$\times \langle \ell_2 \| C^1 \| \ell_2' \rangle \langle \ell_2' \| C^1 \| \ell_2 \rangle \ . \tag{30}$$

The factor $(-1)^{2J}$ is matched by a factor of the same parity when the matrix elements between j_1 and j_1' are further reduced. In the simple case of one bound electron the expression can then be written:

$$A = \frac{2(2j_1+1)(2j_1'+1)}{3\sqrt{2}} \begin{Bmatrix} \frac{1}{2} & \ell_1 & j_1 \\ 1 & j_1' & \ell_1' \end{Bmatrix} \begin{Bmatrix} \frac{1}{2} & \ell_1' & j_1' \\ 1 & j_1 & \ell_1 \end{Bmatrix} \mathrm{Max}(\ell_1, \ell_1') \mathrm{Max}(\ell_2, \ell_2') \ . \tag{31}$$

If the emitting ion is in a close approximation to LS coupling, and the various transitions within a multiplet are unresolved in comparison with the line width, the various $G^{b\beta}$ factors are effectively the same for all values of j_1'

and we may, therefore, sum over this quantum number.

The final result, when we substitute the angular factor back in $T_{ii}^{3(A)}$, is:

$$T_{ii}^{3(A)} = \sum_{b,\alpha\beta} e^4(\gamma_1)^2 \rho_\alpha G^{b\alpha} G^{a\beta} I(a,b) I(\beta,\alpha) R^1(b\alpha,a\beta)$$

$$\times \frac{2(2j_a+1)}{3\sqrt{2}} \frac{\mathrm{Max}(\ell_a,\ell_b)\mathrm{Max}(\ell_\alpha,\ell_\beta)}{(2\ell_a+1)} \quad . \tag{32}$$

In an exactly similar way the angular part of $T_{ii}^{1(C)}$ can be reduced to a final form:

$$A^{1(C)} = \frac{1}{(2k+1)} (2j_1+1)(2j_1'+1)(2j_1''+1)$$

$$\times \begin{Bmatrix} \frac{1}{2} & \ell_1' & j_1' \\ 1 & j_1 & \ell_1 \end{Bmatrix}^2 \times \begin{Bmatrix} \frac{1}{2} & \ell_1'' & j_1'' \\ 1 & j_1' & \ell_1' \end{Bmatrix}^2 \mathrm{Max}(\ell_1,\ell_1')\mathrm{Max}(\ell_1',\ell_1'')\mathrm{Max}(\ell_2,\ell_2') \quad . \tag{33}$$

Carrying out summations over j_1', j_1'' with the assumptions discussed above and substituting into $T_{ii}^{1(C)}$ yields:

$$T_{ii}^{1(C)} = \sum_{b,b',\alpha,\beta,k} e^6(\gamma_1)^2 \rho_\alpha (G_o^{b\alpha})^2 G_o^{b'\beta} (I(a,b))^2 R^k(b\alpha,b'\beta)^2$$

$$\times \frac{(2j_a+1)\mathrm{Max}(\ell_a,\ell_b)\mathrm{Max}(\ell_b,\ell_b')\mathrm{Max}(\ell_2',\ell_2)}{(2k+1)(2\ell_a+1)(2\ell_b+1)} \tag{34}$$

In the case of diagram 1(B) the summation over K and K' finally reduces to a term including:

$$\sum_{K'} (2K'+1)(-1)^{K'+\ell_2+j_1'} \begin{Bmatrix} \ell_2 & j_1' & K' \\ j_1' & \ell_2 & k \end{Bmatrix} = \delta_{k0} \sqrt{(2\ell_2+1)(2j_1'+1)} \quad . \quad (35)$$

But the summation over k is explicitly restricted to $k \geq 1$ from the considerations preceding equation (15). Consequently, so long as the assumptions stated there hold, <u>the contributions of diagrams of type 1(B) vanish</u>[14].

Evaluation of the Cross-Section

The contribution to the cross-section σ at a frequency ω of each of the diagrams is obtained by taking the imaginary part. Since the remainder of the terms are real, it is clear that both cases 1(C) and 3(A) contribute to the cross-section only at the singularity in $G^{b'\beta}(\omega)$ ($b' = a$ in case 3(A)), i.e., when the energy of the perturber in state β is such that:

$$E_a + E_\alpha + \hbar\omega = E_{b'} + E_\beta \quad . \quad (36)$$

The Isolated Line Approximation

We now eliminate the summation over b by making the isolated line approximation; that is, we assume that we are dealing with a system for which at the frequency of interest $G^{ab} = \frac{1}{E_a - E_b + \hbar\omega}$ is appreciable for only one state b. This is, of course, the situation for most lines of non-hydrogenic emitters at moderate densities.

Evaluation of the Radial Integrals, R^k, I, and Summation over Perturber States

The assumption already made that $r_2 > r_1$ allows the generalized Slater Integrals occurring in the expansions given above to be factored into two parts. Thus, for instance:

$$R^k(b\alpha, a\beta) = \int_0^\infty P_a(r_1) r_1^k P_b(r_1) dr_1 \int_0^\infty \frac{F^{\ell\alpha}(K_\alpha r_2)}{K_\alpha} \frac{1}{r_2^{k+1}} \frac{F^{\ell\beta}(K_\beta r_2)}{K_\beta} dr_2 \,. \tag{37}$$

Here $P_a(r_1)$ is the usual radial function for the bound electron, and $F^{\ell\alpha}(K_\alpha r_2)$ is the corresponding solution to the radial equation for a free electron of momentum K_α and and angular momentum ℓ_α (see, e.g., Alder et al.[13], Baranger[10]). Because we have considered only dipole radiation, k = 1 is

the only term contributing to 3(A) and will usually also be very much the dominant term in 1(C).

Thus we are interested in integrals of the form (using the notation of Alder et al.)

$$M^{-2}_{\ell_\alpha,\ell_\beta}(E_\alpha,E_\beta) = \frac{1}{K_\alpha K_\beta}\int_0^\infty F^{\ell_\alpha}(K_\alpha,r_2)\frac{1}{r_2^2}F^{\ell_\beta}(K_\beta r_2)dr_2 \ . \qquad (38)$$

The remaining part of R^k for the bound electron is of just the same form as the integral occurring in the radiation vertex, I.

Case 1(C)

For the case 1(C) the summation over perturber states can then be carried through. The summation over perturber momenta becomes an integral over energies, which leaves a contribution of unity from the principal part integral in $G^{b'\beta}$ and a factor of $\frac{K_\beta m}{(8\pi)^3\hbar^3}$. The remaining summation of $M^{-2}_{\ell_\alpha,\ell_\beta}$ over ℓ_α and ℓ_β can be expressed in terms of the function

$$f(E_\alpha,E_\beta) = \frac{32\pi^2}{9}\,2K_\alpha K_\beta \sum_{\ell_\alpha,\ell_\beta} \mathrm{Max}(\ell_\alpha,\ell_\beta)\,|M^{-2}_{\ell_\alpha\ell_\beta}(E_\alpha,E_\beta)|^2$$

$$= \frac{32\pi^2}{9}\,\frac{\pi}{\sqrt{3}}\,g(E_\alpha,E_\beta) \qquad (39)$$

(Alder[13]) suitably modified[10] for an attractive Coulomb interaction. Substitution in the expression for $T^{1}_{ii}(C)$ above gives a cross section identical to Baranger's[10]:

$$\sigma^{1}(C) = \frac{2}{\hbar F}(\gamma_{1})^{2}e^{6}\sum_{\alpha b'}\frac{1}{V_{\alpha}}\rho_{\alpha}\frac{1}{\hbar}\frac{1}{(E_{a}-E_{b}+\hbar\omega)^{2}}$$

$$\times\frac{(4\pi)^{2}}{3}\frac{(2j_{a}+1)}{(2\ell_{a}+1)}\frac{\mathrm{Max}(\ell_{a},\ell_{b})\mathrm{Max}(\ell_{b},\ell_{b'})}{(2\ell_{b}+1)}$$

$$\times[I(a,b)]^{2}[I(b,b')]^{2}\frac{\pi}{\sqrt{3}}g(E_{\alpha},E_{\beta}) \qquad (40)$$

Diagram 3(A)

The contribution of this diagram contains a single term in $M^{-2}_{\ell_{\alpha}\ell_{\beta}}$ plus a term due to the vertex at which the perturber radiates of the form:

$$I(\beta,\alpha) = \frac{1}{K_{\alpha}K_{\beta}}\int_{0}^{\infty}F^{\ell_{\alpha}}(K_{\alpha}r_{2})r_{2}\,F^{\ell_{\beta}}(K_{\beta}r_{2})dr_{2} = M^{+1}_{\ell_{\alpha}\ell_{\beta}}\,. \qquad (41)$$

Rather than evaluate $I(\beta,\alpha)$ directly we shall relate it to the matrix element $M^{-2}_{\ell_{\alpha}\ell_{\beta}}$ by using the equation of motion for the perturber in the field of the ion's charge[13]:

$$I(\beta,\alpha) = M^{+1}_{\ell_\alpha,\ \ell_\alpha \pm 1}$$

$$= -\frac{Ze^2}{m\ \omega_o^2}\ M^{-2}_{\ell_\alpha,\ \ell_\alpha \pm 1} \qquad (42)$$

Here ω_o is the frequency of the $\alpha \rightarrow \beta$ transition, and is thus approximately the photon energy.

The contribution of 3(A) can now be expressed in a form similar to that of 1(C) by substituting for $I(\beta,\alpha)$ as above. The final result for the cross section is:

$$\sigma^{3(A)} = \frac{2}{\hbar F}\sum_{\alpha}\frac{1}{V}\ e^4\ \rho_\alpha(\gamma_1)^2\ \frac{1}{(E_a - E_b + \hbar\omega)}\ I(a,b)^2\ \frac{(4\pi)^2}{3}$$

$$\times \frac{\pi}{\sqrt{3}}\ g(E_\alpha, E_\beta)\ \frac{Ze^2}{m_o\omega^2}\ \frac{2(2_{ja}+1)\mathrm{Max}(\ell_a,\ell_b)}{\sqrt{2}\ (2\ell_a+1)}\ . \qquad (43)$$

Many-Perturber Treatment

The magnitude of the effects discussed below is such that the one-electron approximation is always adequate. However, to the same order of approximation it is easy to formally incorporate a many-electron treatment by suitably correcting the propagators in the diagrams of Figure 2.

To do this we use the impact-approximation[4,10], that is we assume in evaluating the diagrams that the interactions of separate perturbers do not overlap[8].

Thus, neglecting lower state interactions, we are interested in the following two diagrams:

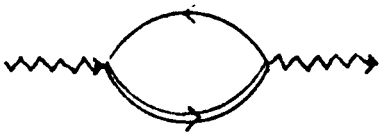

(A)

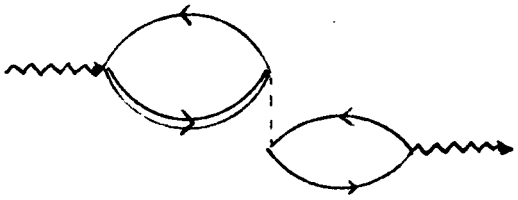

(B)

where the 'exact' bound propagator represented by ⟹ is got from inserting an arbitrary number of self-energy parts into the free propagator line → , i.e.:

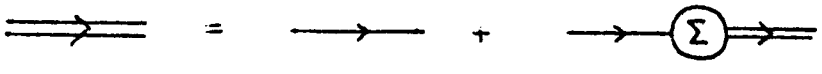

or:

$$\Longrightarrow \;=\; \frac{1}{\rightarrow^{-1} - \Sigma}$$

where $\sum$ is the sum of all diagrams of the type  .

With the appropriate form for 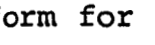 we can now evaluate the two diagrams. Diagram (A) gives a Lorentz profile, thus:

$$\sigma^{(A)} \propto \mathrm{Re}\ \frac{1}{\rightarrow^{-1} - \sum}$$

$$\propto \mathrm{Im}\ \frac{1}{(E_a - E_b + \hbar\omega) + i\Gamma} = \frac{\Gamma}{(E_a - E_b + \hbar\omega)^2 + \Gamma^2} \quad . \tag{44}$$

In the case of diagram (B) we require the <u>real part</u> of since the free electron loop already contributes an extra factor of i. Thus:

$$\sigma^{B} \propto \frac{(E_a - E_b + \hbar\omega)}{(E_a - E_b + \hbar\omega)^2 + \Gamma^2} \tag{45}$$

For $(E_a - E_b + \hbar\omega) >> \Gamma$ this is of the form we have already derived in the one-electron treatment. For $(E_a - E_b + \hbar\omega) < \Gamma$ the contribution of $\sigma(B)$ is proportional to $(E_a - E_b + \hbar\omega)\Gamma^{-1}$, and thus goes to zero at the line center. In other words when the effects of many-perturbers are included, while (A) yields a Lorentz profile, (B) gives a cross section which varies with frequency in the same manner as the refractive

index in the neighborhood of a spectral line.

IV. DISCUSSION

Since in case 1(C) $f(E_\alpha, E_\beta)$ depends upon the particular intermediate state b', we have to specialize somewhat in order to directly compare the contributions of 1(C) and 3(A). We shall consider the particular case where b' = a, i.e., where the perturber induces transitions to the lower state of the optical transition itself. This situation can be of importance in practice, with most, if not all, of the contribution of 1(C) to the cross-section being due to interactions between upper and lower states. A particularly obvious example is the $2s^2S - 2p^2P^\circ$ transition in lithium-like ions, but in many other cases the lower and upper states strongly interact. Another example is the $2p^1P^\circ - 2p^{2\,1}D$ 2296.89 Å transition in C III. Also in many of the cases[1,2] where large discrepancies have been found between the early calculations of Griem[3] and experimental line widths, the b' = a term in the sum over b' contributes up to 50% of the line width.

A direct comparison can then be made between 1(C) and 3(A), since all the factors depending on the initial and intermediate perturber energies are the same in the two cases. When $g(E_\alpha, E_\beta)$ is close to unity diagram 1(D) will contribute an equal amount to that of 1(C), and similarly 3(B), (C), (D) will equal 3(A).

To the order to which we have calculated them, the relative contributions of type 3 and type 1 diagrams will therefore be:

$$\frac{\sigma^3}{\sigma^1} = 2\sqrt{2}\ \frac{Z}{m_o\omega^2}\ \frac{2(\ell_b+1)(E_a-E_b+\hbar\omega)}{[I(a,b)]^2 \mathrm{Max}(\ell_a,\ell_b)} \tag{46}$$

Clearly the type 3 diagrams introduce an asymmetry into the line profile, in comparison with the symmetric profile due to the type 1 cases. Since $(E_a-E_b+\hbar\omega)$ will be of the order of a few line widths, i.e., between 10^{11} and 10^{12} c.p.s. in typical cases at optical frequencies, we see that the asymmetry may vary between much less than 1% and several percent, depending on the particular transition, and on the exact frequency separation from the line center (see specific examples below). For a given transition the percentage asymmetry at a fixed frequency separation from the line

center is independent of the perturber density. Consequently, as the perturber density is raised a given asymmetry will occur at a smaller number of half widths from the line center (the half-width of the Lorentzian component, σ', being proportional to the perturber density), and hence the asymmetry will become more noticeable relative to the peak height of the line.

The overall absorption profile can be written in the form:

$$\sigma^{tot}(\omega) = \sigma^1 + \sigma^2 + \sigma^3$$

$$= C(\omega) + \frac{A+B(\omega-\omega_o)}{(\omega-\omega_o)^2} \qquad (47)$$

where $\omega_o = \frac{E_a - E_b}{\hbar}$

and $C(\omega)$ is the essentially constant contribution of σ^2. The overall profile is the same as the well-known 'resonance,' 'autoionization,' or 'Fano' profile[9], approximated for $(\omega-\omega_o)$ large compared to the half-width.

Since σ^3 can be both negative and larger in absolute magnitude than σ^1 it is necessary to check that $\sigma^{tot} \geq 0$ in the present approximation for all values of $(\omega-\omega_o)$. This

will be so as long as:

$$\frac{\sigma^2}{\sigma^3} \geq \frac{1}{4}\frac{\sigma^3}{\sigma^1} \quad . \tag{48}$$

In fact evaluation of σ^2 easily shows that:

$$\frac{\sigma^2}{\sigma^3} = \frac{3(2\ell_a+1)}{(2\ell_b+1)}\frac{1}{4}\frac{\sigma^3}{\sigma^1} \quad . \tag{49}$$

It is therefore possible for σ^{tot} to be identically zero in the present approximation, but never negative. σ^{tot} can in fact be zero only in the special case when $\ell_a = 0$ (which in any case will turn out to be the most important case for other reasons). This is essentially a consequence of the summation over j_1'' carried out in the angular average of $T_{ii}^{1}(c)$ since exact interference occurs only when a single intermediate state b' is included in σ^1, and b' ≡ a. When $\ell_a \neq 0$ the possible range of j_a increases the importance of σ^1 relative to σ, and σ^{tot} never reaches zero, although it may still be less than the 'background' continuum level, σ^2.

In the special case $\ell_a = 0$, σ^{tot} is zero at a frequency separation from the line center such that $\frac{\sigma^3}{\sigma^1} = -2$. We now consider some particular cases in order to estimate the

magnitude of such frequency separations and to consider the practical implications.

It is clear from the discussion above that such effects will be important only when a) the broadening mechanism involves primarily the interaction of the upper and lower states of the optical transition, and b) the lower state of the optical transition is an S state. This effectively restricts the transitions of interest to those between levels of principal quantum number two, i.e. of the type $2s^m\ 2p^n \rightarrow 2s^{m-1}\ 2p^{n+1}$ (as already mentioned above), apart from some transitions in complex ions where in certain 'accidental' cases the lower state may be the closest interacting level to the upper state of the optical transition (e.g., λ4806, $4s\,^4P - 4p\,^4P$, Ar II).

As specific examples we consider the N II resonance line, λ1085.1 Å, $2s^2\ 2p^2\ ^3P - 2s\ 2p^3\ ^3D^\circ$, the C III λ2296.8 Å $2s\ 2p\ ^1P^3 - 2p^2\ ^1D$ transition, and the C IV λ1549.1 Å resonance line, $2s^2S - 2p^2P^0$. Using the line strengths quoted by Wiese[18] and the usual relations for the line and multiplet factors, we can estimate the transition integral I(a,b), and hence the wavelength separation from the line core at which the asymmetry between blue and red wings is 10% (the blue wing being the stronger). The results are

given in Table I.

The values of $\Delta\lambda$ quoted in the table are extremely large in comparison with the Stark widths of such transitions at the densities found in the more conventional laboratory plasmas (i.e., $n_e = 10^{16} - 10^{17}$ cm^{-3}). However, they are only of the order of the line widths expected at the extreme densities found in some of the newer plasma sources, such as laser-generated plasmas[6] or 'plasma-focus' devices[15], (i.e., $n_e \simeq 10^{20}$ cm^{-3}). Thus the C IV line is expected (from approximate estimates of excitation rates) to have a half-width of the order of a few-tenths of an Angstrom at such densities, and the C III 2296 Å line has been observed to have a half-half width exceeding 5 Å in a plasma generated by focusing a Q-spoilt laser onto a carbon target[16]. In these cases such asymmetries may well be significant. Also it is possible to observe the profile of resonance lines at relevant separations from the line center even in plasmas of much lower densities, if the conditions are such that the optical depth at line-center is large, a technique adopted by Griem and co-workers[17] in obtaining both f-values and damping constants. Interference asymmetries of this sort may therefore be observable at the relatively low densities found in conventional discharges and magnetic compression experiments.

The zero predicted in σ^{total} occurs where $\frac{\sigma^3}{\sigma^1} = -2$, i.e., a factor of 40 further into the line wing than the values of $\Delta\lambda$ given in the table. Clearly this is much greater than the line widths under all conceivable experimental circumstances. However, since the existence and position of this zero is independent of perturber density (as is the line-to-continuum ratio at large distances in the line wing), this effect may be observable even under conditions in which the Stark width of the line of interest is extremely small. For the C III line this effect will always be negligible, since the lower state of the transition is not the ground state of the ion, and thus contributes negligibly to the total underlying continuum intensity. Similarly in many experimental situations the continuum intensity may be due to other species of ion, frequently, of course, to protons, and the continuum intensity due to a small-concentration impurity of some particular ionic species will not be observable. However, in the two particular experimental situations mentioned above the circumstances may be very different. Under appropriate temperature conditions in laser-generated plasmas the continuum-intensity near a resonance transition may be largely or entirely due to Bremsstrahlung from electrons interacting with ions in the

ground state of the same resonance transition. The same may be true in plasma-focus devices if operated in gases other than hydrogen, or even if the ion of interest is present as a small-concentration impurity, since the extreme values of ion-charge which can be reached ($Z > 18$) can result in the Bremsstrahlung from such small concentration but highly ionized impurities entirely dominating that due to protons or deuterons. The difficulty in rapidly stripping Li-like ions in such transient devices will also tend to ensure that a significant percentage of the total ion concentration is in this stage. In these cases significant deviations from the continuum intensity expected on a fully-stripped ion model may occur in the vicinity of resonance transitions of the type discussed above.

CONCLUSIONS

The consequences of the usual neglect, in theories of electron-impact broadening, of radiation due to the perturbing electrons have been investigated. Inclusion of the dipole-radiation due to the perturber results in an interference effect, as well as the normal Bremsstrahlung radiation. This interference produces an asymmetry of the

impact-broadened profiles of resonance lines, especially the $2s^2S - 2p^2P^\circ$ transitions of Li-like ions, and under particular circumstances, may produce a strong interference dip in the continuum intensity on the red-side of the line.

The interference effect is not significant, in so far as the line-profile is concerned, unless the major broadening mechanism involves the direct interaction of the upper and lower states of the line of interest, and even then the resulting asymmetries are small at normal densities. However, at the extreme densities found in laser-generated plasmas, such effects may well be observable and important, as they may be also at lower densities if the extreme wings of optically thick lines are observed. The deviation of the continuum intensity from the simple theory may also be observable even at low densities. Such interference effects may also be important in determining the profiles of low-frequency transitions between excited states of heavy ions, in view of the explicit dependence on ω in Eqn. (45).

In addition such asymmetries may perhaps be relevant in interpreting in detail the ultra-violet spectra of early-type stars, e.g., those studied by Morton[19], where lines such as C IV $2s^2S - 2p^2P^\circ$ are both observed in abosrption, and are expected theoretically to be strong several Angstroms into the wings.

Acknowledgements

This work was supported by NASA Grant (NsG-438) at NGL-22-007-006 Harvard College Observatory while the author was on leave-of-absence from Imperial College. I wish to thank Professor L. Goldberg and the many other people at Harvard College Observatory who have offered hospitality and scientific advice during my stay. In particular I am indebted to Dr. B.W. Shore for many helpful and stimulating discussions and to Professor A. Dalgarno for reading the manuscript of this paper.

References

1. J. Cooper and G.K. Oertel, Phys. Rev. Letts., 18, 985, 1967.
2. H.R. Griem, Phys. Rev. 165, 258, 1967.
3. H.R. Griem, Plasma Spectroscopy, McGraw Hill Publishers 1964.
4. J. Cooper, Phys. Rev. Letts., 17, 991, 1966.
5. H.R. Griem, Phys. Rev. Letts. 17, 509, 1966.
6. D.D. Burgess, B.C. Fawcett and N.J. Peacock, Proc. Phys. Soc., 92, 805, 1967.
7. E.W. Smith and C.F. Hooper, Phys. Rev. 157, 126, 1967.
8. B. Bezzerides, J. Quant. Specty. Radiative Transfer 7, 353, 1967.
9. B.W. Shore, Rev. Mod. Phys., 39, 439, 1967.
10. M. Baranger, Atomic and Molecular Processes, Academic Press, 1962 and M. Baranger and J.C. Stewart, General Atomic Report, G AMD-996.
11. R.D. Mattuck, A Guide to Feynman Diagrams in the Many-Body Problem, McGraw Hill Publishers, 1967.
    D.J. Thouless, The Quantum Mechanics of Many-Body Systems, Academic Press, 1961.
12. B.W. Shore and D.H. Menzel, Principles of Atomic Spectra, Wiley and Sons Inc., Publishers, 1968.

A.R. Edmonds, Angular Momentum in Quantum Mechanics, Princeton University Press, 1960.

13. K. Alder, A. Bohr, T. Huus, B. Mottelson and A. Winther, Rev. Mod. Phys. 28, 432, 1956.

14. In a sense this result is equivalent to Furry's theorem in Quantum Electrodynamics, and could be predicted directly by realizing that the angular momenta involved can be represented graphically in a way topologically equivalent to the Feynman diagram for the interactions. See e.g. B.R. Judd, Second Quantization and Atomic Spectroscopy, John Hopkins Press, Baltimore, 1967, for references and further discussion.

15. J.W. Long, N.J. Peacock, P.D. Wilcock and R.J. Speer, Abstract C5, Topical Conference on Pulsed High-Density Plasmas, Bulletin of the American Phys. Society 12, No. 8, 1967.

16. D.D. Burgess and N.J. Peacock, Unpublished results.

17. R. Lincke and H.R. Griem, Phys. Rev. 143, 66, 1966.

18. W.L. Wiese, M.W. Smith and B.M. Glennon, NSRDS-NBS4 Vol. 1, Atomic Transition Probabilities, U.S. Govt. Printing Office 1966.

19. D.C. Morton, Ap. J., 147, 1017, 1967, and Ap. J., 141, 73, 1965.

Ion	Transition	Wavelength	Line Strength, S (Atomic Units)	$[I(a,b)]^2$ (Atomic Units)	$\Delta\lambda$ for 10% Asymmetry
N II	$2s^2 2p^2\,{}^3P\text{-}2s2p^3\,{}^3D^\circ$	1085.1 Å	2.5 A.U.	4.55 A.U.	12.5 Å
C III	$2s2p^1P^\circ\text{-}2p^2\,{}^1D$	2296.9 Å	11.0 A.U.	3.20 A.U.	4.4 Å
C IV	$2s^2S\text{-}2p^2P^\circ$	1549.1 Å	1.9 A.U.	1.43 A.U.	1.3 Å

(N.B.; (a,b) in Eqs. 44 is in cm).

Table 1: Estimated Wavelength Separations from Line Center for Asymmetry between Blue and Red Wings.

Figure Captions

Figure 1: Diagrammatic representation of contributions to T_{ii} through second order in V^{int}.

Figure 2: Bubble diagram representation of the diagonal T-matrix elements shown in Figure 1.

Figure 3: One of many diagrams constructed from free particle (i.e. plane wave) propagators which contribute to diagrams 3(A), (D) in Figure 2.

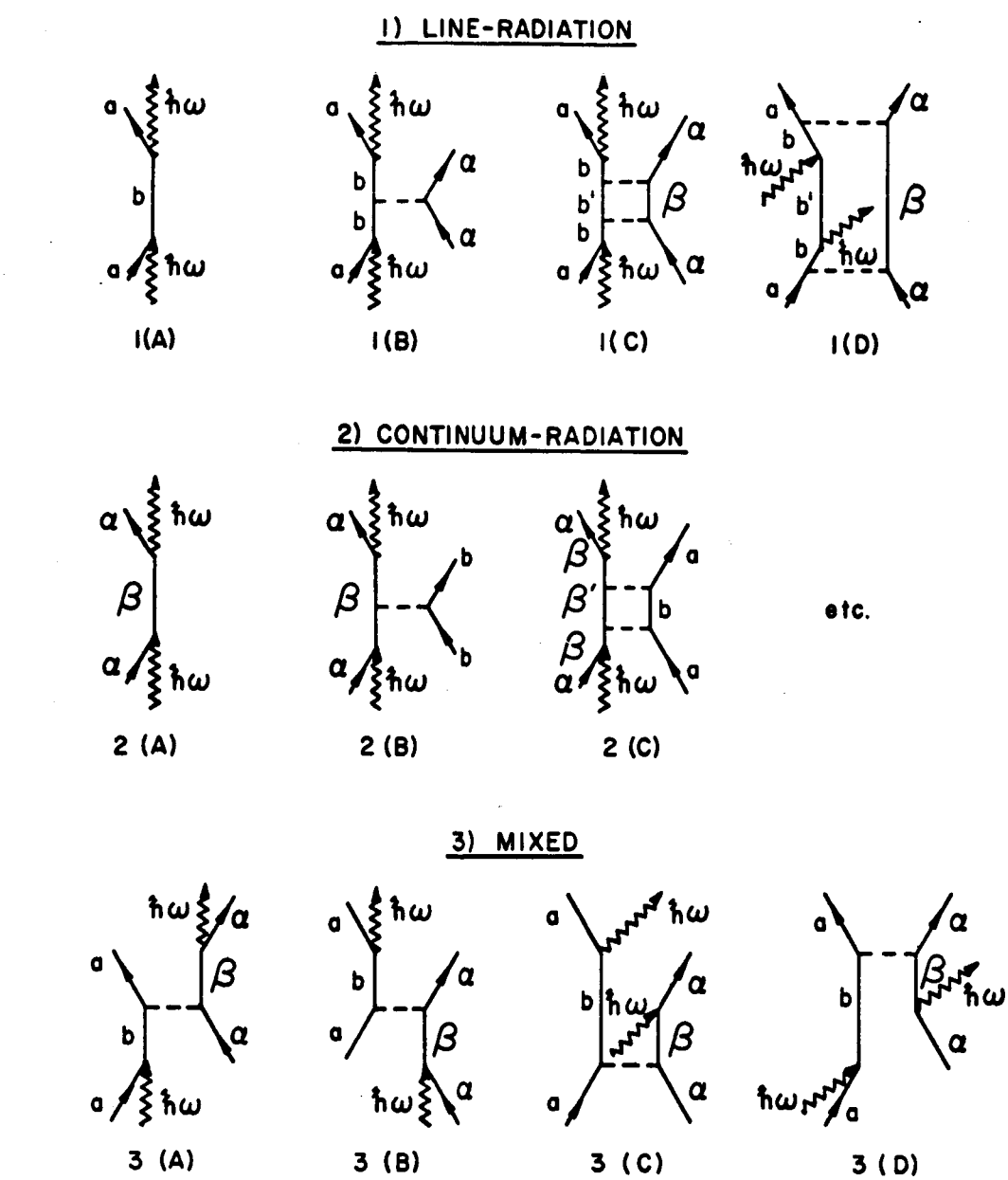
1) LINE-RADIATION
1(A)
1(B)
1(C)
1(D)
2) CONTINUUM-RADIATION
2 (A)
2 (B)
2 (C)
etc.
3) MIXED
3 (A)
3 (B)
3 (C)
3 (D)
a —— BOUND ELECTRON
α —— FREE ELECTRON
ħω ~~~ PHOTON

FIGURE 1

1) LINE-RADIATION

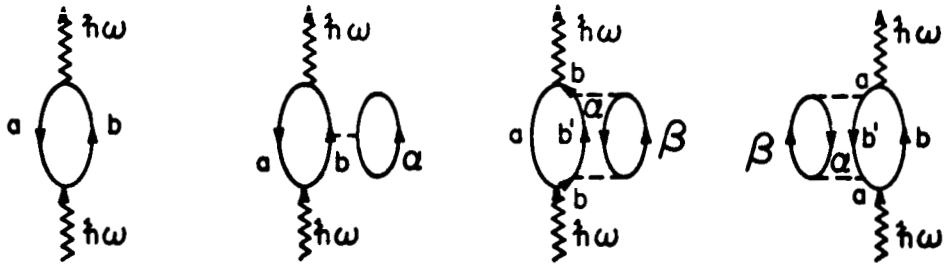

I (A) I (B) I (C) I (D)

2) CONTINUUM-RADIATION

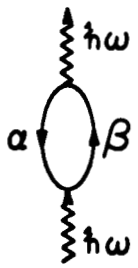

2 (A)

etc.

3) MIXED

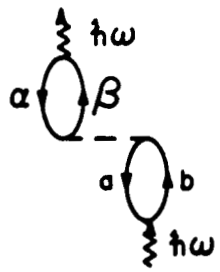

3 (A), (D)

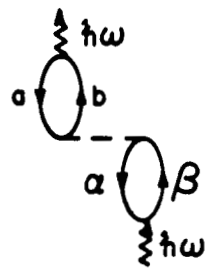

3 (B), (C)

FIGURE 2

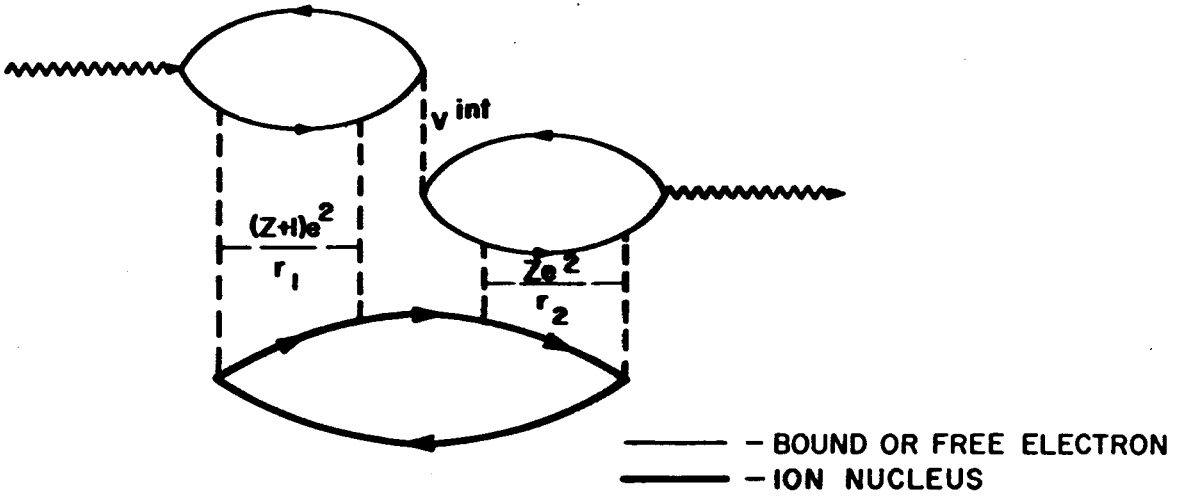

FIGURE 3